

1                   **CNTs-added PMNT/PDMS flexible piezoelectric nanocomposite**  
2                   **for energy harvesting application**

3           Napatporn Promsawat<sup>1</sup>, Methee Promsawat<sup>2</sup>, Phatthanapong Janphuang<sup>3</sup>, Zhenhua Luo<sup>4</sup>,  
4           Steve Beeby<sup>5</sup>, Catleya Rojviriyaya<sup>3</sup>, Phakkhananan Pakawanit<sup>3</sup> and Soodkhet Pojprapai<sup>1</sup>

5                   <sup>1</sup>School of Ceramic Engineering, Institute of Engineering, Suranaree University of  
6                   Technology, Nakhon Ratchasima,30000, Thailand

7                   <sup>2</sup>Department of Materials Science and Technology, Faculty of Science, Prince of Songkla  
8                   University, Songkhla, 90112, Thailand

9                   <sup>3</sup>Synchrotron Light Research Institute, 111 University Avenue, Muang District, Nakhon  
10                   Ratchasima, 30000, Thailand

11                   <sup>4</sup>School of Water, Energy and Environment, Cranfield University, Cranfield MK43 0AL, UK

12                   <sup>5</sup>Electronics and Computer Science, University of Southampton, SO17 1BJ, UK

13                   \*Corresponding author. Email: soodkhet@g.sut.ac.th (S. Pojprapai)

14           **Abstract**

15           The flexible piezoelectric nanocomposites based on lead magnesium niobate titanate  
16           [Pb(Mg<sub>1/3</sub>Nb<sub>2/3</sub>)<sub>0.65</sub>Ti<sub>0.35</sub>O<sub>3</sub>; PMNT] particles in polydimethylsiloxane (PDMS) matrix were  
17           fabricated and characterized. PMNT powders are synthesized using the columbite precursor  
18           method. PMNT/PDMS flexible nanocomposites are then prepared by spin casting technique,  
19           where a small amount of carbon nanotubes (CNTs) is added into the PMNT/PDMS composite  
20           to enhance cross-links between PMNT particles and PDMS matrix. The phase and  
21           microstructure of the nanocomposite are investigated by using X-ray diffraction and scanning  
22           electron microscope (SEM). The electromechanical behavior is evaluated by using an

1 autonomous pneumatic actuator. The flexible composite, occupying approximately 300 mm<sup>2</sup>,  
2 is capable of generating an open-circuit voltage ( $V_{oc}$ ) of  $2.83\pm 0.24$  V and a short-circuit current  
3 ( $I_{sc}$ ) signal of  $0.33\pm 0.01$   $\mu$ A across 10  $\Omega$  resistor under mechanical load of 300 N. The  
4 generated electrical charges are 29026 pC. The relative dielectric constant is measured at 10  
5 kHz and found to be  $6.76\pm 1.15$ . The piezoelectric PMNT/PDMS composite can be potentially  
6 used in a variety of applications such as wearable sensors, actuators, and energy harvesting for  
7 converting kinetic energy into useful electrical energy.

8 **Keywords:** PMNT, polydimethylsiloxane (PDMS), carbon nanotube, nanocomposite, energy  
9 harvesting

10

## 11 **1. Introduction**

12 Nowadays, renewable energy such as solar, vibrations, electromagnetic wave and thermal  
13 energy are widely used in technological applications. These ambient energies have been  
14 received much attention from many researchers for applications in the energy conversion  
15 technology. The ambient energy sources can be converted to electrical energy via energy  
16 conversion processes, i.e. electromagnetic induction [1-2], triboelectric generator [3],  
17 electrostatic transduction [4], or using energy conversion materials, e.g., electroactive  
18 ferroelectret [5] and piezoelectric materials [6]. Piezoelectric materials are one of the energy  
19 conversion materials that can convert kinetic energy from mechanical vibrations to electrical  
20 energy via direct piezoelectric effect. Vice versa, they can convert electrical energy to  
21 mechanical strain, which is called the converse piezoelectric effect. Using the direct effect,  
22 piezoelectric materials can be used to harvest kinetic energy generated from human activities  
23 (e.g. walking and running). To date Pb-based piezoelectric materials are the most used in  
24 applications due to their high electromechanical coupling factor ( $k$ ) and stimulating at  
25 resonance frequencies could realize an energy conversion efficiency above 80% [7]. Of these,

1 lead magnesium niobate titanate (PMNT) materials is of great interest due to their high  
2 electromechanical coupling coefficient which make them as one of promising solution for  
3 piezo-sensors and actuators applications [8-9]. The composition of PMNT are typically  
4  $\text{Pb}(\text{Mg}_{1/3}\text{Nb}_{2/3})_{1-x}\text{Ti}_x\text{O}_3$  and it is well-known as relaxor-based ferroelectric material. The  
5 composition with  $x = 0.30-0.35$  is at morphotropic phase boundary (MPB) region  
6 demonstrating best piezoelectric properties [10]. However, the ceramic form of these PMNT  
7 materials is brittle and heavy, making them unsuitable for flexible devices. This disadvantage  
8 can be overcome by flexible piezoelectric ceramic-polymer composite [11-12]. The particle  
9 size of ceramic powder in the composite is one of the main factors that could affect the  
10 piezoelectric properties of the composite. Nevertheless, there were a few works studying the  
11 effect of the size of piezoelectric particles on piezoelectric properties of the flexible  
12 piezoelectric composites. For example, the work studied by Lee *et al.* reported that the  
13 dielectric and piezoelectric constants of the piezoelectric composite with  $\text{PbTiO}_3$  as the  
14 piezoelectric phase increased as the size of the piezoelectric particle increased [13]. Although  
15 most polymers exhibit poor piezoelectric properties and dielectric constant, their high  
16 flexibility, and forming and shaping abilities make them suitable to be a matrix phase for  
17 piezoelectric composites [14-15]. To fabricate piezoelectric ceramic-polymer composite,  
18 Polydimethylsiloxane (PDMS) was frequently used as a polymeric matrix due to its flexibility,  
19 biocompatibility, and optical transparency. Importantly, it is cost-effective, low toxicity, low  
20 permeability to water, high oxidative and high thermal stability [16-18]. Recently, Park *et al.*  
21 developed a flexible nanocomposite generator based on PZT particles distributing in a PDMS  
22 matrix with added CNTs [19]. The output voltage and current signals of the device were 10 V  
23 and 1.3  $\mu\text{A}$ . Furthermore,  $\text{NaNbO}_3$  nanowires-PDMS composites with output voltage and  
24 current of 3.2 V and 72 nA have been synthesized by Jung *et al.* [20]. Chen *et al.* fabricated  
25 piezoelectric nanogenerators based on PZT nanofibers which generated the output voltage and

1 power under periodic stress application of 1.63 V and 0.03  $\mu\text{W}$ , respectively [21]. Jeong *et al.*  
2 successfully produced lead-free flexible nanocomposite generators by a simple spin-casting  
3 method. The output voltage and current signals, which were generated during repeated bending  
4 and unbending motions with a maximum displacement of 5 mm at a rate of  $0.2 \text{ m s}^{-1}$ , were 12  
5 V and  $1.2 \mu\text{A}$ , respectively [22]. To date, based on our knowledge, only few studies have been  
6 reported on flexible piezoelectric composite based on PMNT in PDMS matrix [23-25].

7 In this work, flexible piezoelectric composites based on  $\text{Pb}(\text{Mg}_{1/3}\text{Nb}_{2/3})_{0.65}\text{Ti}_{0.35}\text{O}_3$  (PMNT)  
8 particles dispersed in PDMS polymeric matrix were fabricated. 1wt% CNTs was added into  
9 the composite in order to improve the electrical conductivity path between micron-sized  
10 piezoelectric particles while maintaining the domain switching during poling process. Physical  
11 and electromechanical properties such as phase, microstructure, dielectric properties, and  
12 power output of the fabricated composite were then characterized in order to obtain more  
13 detailed description of the piezoelectric nanocomposite.

## 14 2. Experimental Details

15  $\text{Pb}(\text{Mg}_{1/3}\text{Nb}_{2/3})_{0.65}\text{Ti}_{0.35}\text{O}_3$  (PMNT) powders employed as the dispersed phase in this research  
16 were prepared by the columbite precursor method from  $\text{PbO}$ ,  $\text{MgO}$ ,  $\text{Nb}_2\text{O}_5$  and  $\text{TiO}_2$  precursors  
17 [25]. Firstly,  $\text{MgO}$  and  $\text{Nb}_2\text{O}_5$  powders were mixed and then calcined at  $900 \text{ }^\circ\text{C}$  for 4 hr to  
18 produce columbite ( $\text{MgNb}_2\text{O}_6$ ) powders. The  $\text{MgNb}_2\text{O}_6$  powder was then mixed with  $\text{PbO}$  and  
19  $\text{TiO}_2$  powders and calcined at  $850 \text{ }^\circ\text{C}$  for 2 h to produce PMNT powders. Polydimethylsiloxane  
20 (PDMS) Sylgard 184 from Dow Corning was used as the matrix phase. PDMS elastomer was  
21 mixed with a curing agent using the weight ratio between the elastomer and the curing agent  
22 of 10:1. The mixture was exposed to thermal curing in order to harden PDMS. 12 wt% PMNT  
23 particles were dispersed in the PDMS elastomer in a beaker. After that, 1 wt% CNTs  
24 ( $\text{NANOCYL}^{\text{TM}}$  NC7000) was added into the mixture and desiccated under vacuum for 20-30  
25 min to remove air bubbles formed during the mixing process. The layered composites, as

1 shown in Fig. 1(a), were fabricated by the following steps; (i) spinning PDMS polymer onto a  
2 glass plate and then curing at 85 °C for 1 h in an oven (ii) spinning CNTs-added PMNT/PDMS  
3 mixture onto the PDMS layer and then curing at 85 °C for 1 h in an oven and (iii) spinning  
4 PDMS polymer onto the mixture layer and then curing at 85 °C for 24 h in an oven. After these  
5 steps, a flexible piezoelectric composite with a thickness in the range of 200-300  $\mu\text{m}$  was  
6 achieved as illustrated in Fig. 1(b). Both sides of the layered composite were etched by oxygen  
7 plasma before electrodes were deposited. The silver electrodes were sputtered on plastic  
8 substrates (200  $\mu\text{m}$  in thickness) and attached onto the etched surfaces using unsolidified  
9 PDMS as a binder. The composite electrodes were cured in an oven at 85 °C for 1 h. Each  
10 composite sample was poled under an applied DC electric field of 2.5 kV/mm at 80 °C for 15  
11 h in silicon oil bath. An electrical poling process was required to align the dipole moment to  
12 the same direction and to enhance piezoelectric properties of flexible nanocomposite devices.  
13 The phases of samples were identified by X-ray diffraction (XRD) technique (Bruker D8  
14 Advance) with Cu  $K_{\alpha}$  radiation wavelength of 1.54 Å. Frequency dependence of a dielectric  
15 constant ( $\epsilon_r$ ) and loss tangent ( $\tan\delta$ ) was measured using a LCR meter (GW INSTEK LCR-  
16 821). Microstructure was observed by a field emission scanning electron microscope (FE-  
17 SEM, JEOL JSM-7800F). Chemical composition was analyzed by an energy dispersive X- ray  
18 spectroscopy (EDX). The internal distribution of the dispersed and matrix phases was  
19 investigated using synchrotron X-ray computed tomography. The synchrotron X-ray beam  
20 with energy range of 2-18 keV (white beam) was scanned on the sample. The  
21 Electromechanical behavior of the composites was investigated using an in-house developed  
22 autonomous pneumatic actuator. The output voltage and current under mechanical load were  
23 measured using an oscilloscope (Tektronix MSO 3034) and a multi-meter (Agilent 34461A).

### 24 3. Results and Discussion

1 X-ray diffraction patterns of PMNT powder, PDMS polymer, and PMNT/PDMS  
2 nanocomposite are shown in Fig. 2. It is obvious that the XRD pattern of the PMNT powder  
3 was well-matched with the ICSD file No. 157487 of  $\text{Pb}(\text{Mg}_{1/3}\text{Nb}_{2/3})_{0.65}\text{Ti}_{0.35}\text{O}_3$  compound with  
4 tetragonal  $P4mm$  space group. No secondary phase was observed on the pattern. The XRD  
5 pattern of the PDMS indicated an amorphous phase of the sample. A broad peak at  $2\theta \approx 12^\circ$   
6 was found, which is consistent with the previous observation of Niu *et al.* [27]. In addition, for  
7 the composite, unknown peaks were observed at  $2\theta \approx 28^\circ$ . The unknown peaks were believed  
8 to be possessed by  $\text{Pb}_{1.83}\text{Nb}_{1.71}\text{Mg}_{0.29}\text{O}_{6.39}$  pyrochlore phase (JCPDS file No. 33-0769). The  
9 splitting of (002) and (200) peaks at  $2\theta \approx 45^\circ$  was also presented. None of CNTs pattern was  
10 observed in the composite. Since only 1 wt% CNTs was added, it is likely that such small  
11 amount was below the detection limit of the XRD apparatus.

12 SEM images of a cross-sectional view of a composite is shown in Fig. 3(a). The layer of the  
13 CNTs-added PMNT/PDMS material with  $203.58 \pm 1.96 \mu\text{m}$  of thickness was observed in the  
14 middle region of the composite sandwiched by the PDMS layers. It can be seen from Fig. 3(b)  
15 that the particle size of PMNT phase was about  $3 \mu\text{m}$ . It was clear that CNTs bridged PMNT  
16 particles to the matrix, as indicated by the arrow in Fig. 3(b) and (c). This contributed to an  
17 improvement of a transportation of charge carriers between the dispersed phase and the matrix  
18 phase while maintaining domain switching in a poling process. This could be confirmed by a  
19 result observed by Gong *et al.*, that the applied field amplitude used in poling CNTs-added  
20 composite was lower than the composition without CNTs [28]. A synchrotron X-ray image of  
21 CNTs added PMNT/PDMS composite is shown in Fig. 3(d). The different contrast is depended  
22 on the level of X-ray absorption of each phase composed in the composite. As shown in the  
23 figure, the dark and bright regions represented the locations of the PMNT and PDMS phases,  
24 respectively. The brightest region indicated the position at which voids or porosities were  
25 located, resulting in a reduction of X-ray absorption at those positions of materials. By using

1 the synchrotron X-ray imaging technique, the dispersion of PMNT particles in PDMS polymer  
2 matrix can be determined. It was also found from the figure that the average size of the dark  
3 region was about 30  $\mu\text{m}$ . This indicated the agglomeration of PMNT particles. Although the  
4 particle size of PMNT was small, the agglomeration of the PMNT particles and the bridging  
5 between the dispersed and the matrix phases of CNTs could contribute to a good piezoelectric  
6 properties of the composite. Energy dispersive X-ray spectroscopy (EDX) of CNTs-added  
7 PMNT/PDMS nanocomposite was shown in Fig. 4(a) and (b). The results clearly showed the  
8 present of Pb, Mg, Nb, Ti and O peak in the PMNT particles and showed C peak representing  
9 local CNTs.

10 Frequency dependences of relative permittivity ( $\epsilon_r$ ) and dielectric loss ( $\tan\delta$ ) measured at  
11 room temperature of CNTs-added PMNT/PDMS nanocomposite is shown in Fig. 5. The result  
12 showed that  $\epsilon_r$  of the composite suddenly decreased while  $\tan\delta$  increased when frequency  
13 increased from 1 kHz to 10 kHz and it decreases when the frequency is greater than 10 kHz.  
14 The decreasing tendency with frequency of dielectric constant could be caused by an interfacial  
15 relaxation. The interfacial polarization arise as a result of difference in conducting phases, but  
16 was interrupted at grain boundaries due to lower conductivity. Generally, in polycrystalline  
17 materials, the grain exhibits semi-conducting behavior while the grain boundary is insulator.  
18 At higher frequency, the charge carriers will no longer be able to rotate sufficiently rapidly, so  
19 their oscillation will be laid behind the field resulting in a decrease of dielectric permittivity  
20 [29]. The dielectric losses at low frequencies are much higher than those occurring at high  
21 frequencies. However, the permittivity of the composite is still above 5. It was found in a  
22 previous result observed by Du *et al.* that a monolithic PDMS and PDMS based materials  
23 showed dielectric constant in the range of 2.32-2.40 [30]. Furthermore, Romasanta *et al.* [31]  
24 reported that the nanocomposite containing 1.0 wt% of CNT influenced to electrical insulator  
25 behavior with a permittivity constant of 1.5 times. It is ascribed to the motion of free charge

1 carriers due to the formation of a continuous conductivity pathway throughout the medium  
2 between CNTs. Therefore, it could imply that an addition of PMNT and CNTs improves  
3 dielectric properties of PDMS polymers.

4 The electrical characterization of PMNT/PDMS nanocomposites with an area of 30 mm ×  
5 10 mm is illustrated in Fig. 6(a). The output voltage and generated current under an applied  
6 mechanical load of 300 N were about of  $2.83 \pm 0.24$  V and  $0.33 \pm 0.01$   $\mu$ A. The calculated output  
7 power of this device is 0.934  $\mu$ W at load resistance of 10 ohm. As compared to the piezoelectric  
8 generators in literature [20,32,33], it was found that the output power of our nanocomposite  
9 was lower than that of the flexible PZT-based composite, which is equal to 13  $\mu$ W, but higher  
10 than those of the BaTiO<sub>3</sub> thin film and NaNbO<sub>3</sub> nanowires-PDMS composite piezoelectric  
11 generators, which are equal to 0.026 and 0.23  $\mu$ W. Fig. 6(b) showed the output current versus  
12 time of the composite. The charge generated by the composite can be determined by integrating  
13 the current over the time. Using an applied force of 300 N, the average generated charge was  
14 equal to 29026 pC. By dividing the charge with the force, the piezoelectric constant ( $d_{33}$ ) of the  
15 composite was calculated which was about 97 pC/N. Moreover, with the permittivity measured  
16 at 1 kHz of 10.5, the piezoelectric voltage constant ( $g_{33}$ ) was calculated to be about 1.04 V·m/N.  
17 As compared to PZT/PDMS composites prepared in the previous works by Babu *et al.* [33]  
18 and Sharma *et al.* [34] at the equivalent amount of the piezoelectric elements (~ 2 vol%), it was  
19 found that our CNTs-added PMNT/PDMS nanocomposite showed higher  $d_{33}$  and  $g_{33}$ . The  $d_{33}$   
20 and  $g_{33}$  values of the PZT/PDMS composites were below 40 pC/N and 50 mV·m/N,  
21 respectively. The greater of piezoelectric properties of CNTs-added PMNT/PDMS  
22 nanocomposite is possibly due to two contributions; 1) low coercive field ( $E_c \sim 7$  kV/cm) with  
23 large remanent polarization ( $P_r \sim 31$   $\mu$ C/cm<sup>2</sup>) of the PMNT material [26] and 2) bridging a  
24 PMNT particle to the neighboring particles and PMNT particles to PDMS matrix by added



1 CNTs. These could allow most dipole moments of PMNT phase to switch their directions to  
2 the direction of applied field in the poling process.

#### 3 **4. Conclusion**

4 CNTs-added PMNT/PDMS flexible nanocomposites have been successfully fabricated. The  
5 electrode was prepared by sputtering silver onto plastic substrate. Both sides of the composite  
6 were etched by oxygen plasma before electrodes were attached. XRD pattern of the composite  
7 indicated PMNT phase and PDMS phase. PMNT particles were dispersed around in PDMS  
8 polymer matrix and bridged the neighboring particles and PDMS polymer by CNTs. Dielectric  
9 permittivity and loss tangent of the composite almost decreased with an increase in frequency.  
10 The voltage and current output were found to be  $2.83 \pm 0.24$  V and  $0.33 \pm 0.01$   $\mu$ A, equivalent to  
11  $0.934$   $\mu$ W. Under an applied force of 300 N, the composite generated the electrical charge of  
12 29,026 pC. The calculated piezoelectric and voltage constants were 97 pC/N and 1.04 V·m/N,  
13 respectively. The use of CNTs as a bridging conductive material could facilitate a poling  
14 performance, thereby improving piezoelectric properties of CNTs-added PMNT/PDMS  
15 nanocomposites which are suitable for flexible electronic devices and sensor applications.

16

#### 17 **Acknowledgments**

18 This work was supported by Suranaree University of Technology (SUT) and the Higher  
19 Education Research Promotion and National Research University Project of Thailand, Office  
20 of the Higher Education Commission. The technologies have been developed at School of  
21 Ceramic Engineering – SUT in collaboration with BL6a: Deep X-ray Lithography and  
22 BL1.2W: X-ray Imaging & Microtomography, Synchrotron Light Research Institute (Public  
23 Organization).

#### 24 **References**

- 1 [1] Beeby SP, Torah RN, Tudor MJ, Glyne-Jones P, O' Donnell T, Saha CR and Roy S: A  
2 micro electromagnetic generator for vibration energy harvesting. *J Micromech Microeng.*  
3 2007;17: 1257-1265.
- 4 [2] Niroomand M and Foroughi HR: A rotary electromagnetic microgenerator for energy  
5 harvesting from human motions. *J Appl Res Technol.* 2016;14: 259-267.
- 6 [3] Wang ZL: Triboelectric Nanogenerators as New Energy Technology for Self-Powered  
7 Systems and as Active Mechanical and Chemical Sensors. *ACS NANO.* 2013;14: 9533-  
8 9557.
- 9 [4] Arya S, Khan S and Lehana P: Design and fabrication of electrostatic micro-cantilever  
10 array as audible frequency generator. *J Electrostat.* 2015;76: 145-151.
- 11 [5] Shi J, Zhu D and Beeby SP: An investigation of PDMS structures for optimized  
12 ferroelectret performance. *J Phys Conf Ser.* 2014;557: 012104.
- 13 [6] Cho JY, Jeong S, Jabbar H, Song Y, Ahn JH, Kim JH, Jung HJ, Yoo HH and Sung TH:  
14 Piezoelectric energy harvesting system with magnetic pendulum movement for self-  
15 powered safety sensor of trains. *Sens Actuators A.* 2016;250: 210-218.
- 16 [7] Wang X: Piezoelectric nanogenerators- Harvesting ambient mechanical energy at the  
17 nanometer scale. *Nano Energy.* 2012;1: 13-24.
- 18 [8] Arai T, Ohno T, Matsuda T, Sakamoto N, Wakiya N and Suzuki H: Synthesis and  
19 electrical properties of  $\text{Pb}(\text{Mg}_{1/3}\text{Nb}_{2/3})\text{O}_3$ - $\text{PbTiO}_3$  epitaxial thin films on Si wafers using  
20 chemical solution deposition. *Thin Solid Films.* 2016;603: 97-102.
- 21 [9] Liang Z, Pei S, Qin F, Zheng Y, Zhao H, Zhang Z, Zeng J, Ruan W, Li G and Cao W:  
22  $\text{Er}^{3+}$  doped ferroelectric  $\text{Pb}(\text{Mg}_{1/3}\text{Nb}_{2/3})\text{O}_3$ -0.25 $\text{PbTiO}_3$  ceramic used as a linear response  
23 fluorescent temperature sensor. *J Lumin.* 2017;181: 128-132.

- 1 [10] La-Orauttapong D, Noheda B, Ye ZG, Gehring MP, Toulouse J, Cox DE and Shirane G:  
2 Phase diagram of the relaxor ferroelectric  $(1-x)\text{Pb}(\text{Zn}_{1/3}\text{Nb}_{2/3})\text{O}_3-x\text{PbTiO}_3$ . *Phys Rev B*.  
3 2002;65: 144101.
- 4 [11] Janas VF and Safari A: Overview of Fine- Scale Piezoelectric Ceramic/ Polymer  
5 Composite Processing. *J Am Ceram Soc*. 1995;78: 2945-2955.
- 6 [12] Banerjee S and Cook-Chennault KA: An investigation into the influence of electrically  
7 conductive particle size on electromechanical coupling and effective dielectric strain  
8 coefficients in three phase composite piezoelectric polymers. *Composites, A*. 2012;43:  
9 1612-1619.
- 10 [13] Lee MH, Halliyal A and Newnham RE: Poling of Coprecipitated Lead Titanate-Epoxy  
11 0-3 Piezoelectric Composites. *J Am Ceram Soc*. 1989;72: 986-990.
- 12 [14] Di C, Xue S, Tong J and Shi X: Study on electromechanical characterization of  
13 piezoelectric polymer PVDF in low-frequency band. *J Mater Sci Mater Electron*. 2014;25:  
14 4735-4742.
- 15 [15] Wang T, Farajollahi M, Choi YS, Lin IT, Marshall JE, Thompson NM, Kar-Narayan S,  
16 Madden JDW and Smoukov SK: Electroactive polymers for sensing. *Interface Focus*.  
17 2016;6: 20160026.
- 18 [16] Zhang H and Chiao M: Anti-fouling Coatings of Poly(dimethylsiloxane) Devices for  
19 Biological and Biomedical Applications. *J Med Biol Eng*. 2015;35: 143-155.
- 20 [17] Dahiya R, Gottardi G and Laidani N: PDMS residues-free micro/macrostructures on  
21 flexible substrates. *Microelectron. Eng*. 2015;136: 57-62.
- 22 [18] Chenoweth K, Cheung S, Duin ACTV, Goddard III WA and Kober EM: Simulations on  
23 the Thermal Decomposition of a Poly(dimethylsiloxane) Polymer Using the ReaxFF  
24 Reactive Force Field. *J Am Chem Soc*. 2005;127: 7192-7202.

- 1 [19] Park KI, Jeong CK, Ryu J, Hwang GT and Lee KJ: Flexible and Large- Area  
2 Nanocomposite Generators Based on Lead Zirconate Titanate Particles and Carbon  
3 Nanotubes. *Adv Energy Mater.* 2013;3: 1539-1544.
- 4 [20] Jung JH, Lee M, Hong JL, Ding Y, Chen CY, Chou LJ and Wang ZL: Lead-Free  $\text{NaNbO}_3$   
5 Nanowires for a High Output Piezoelectric Nanogenerator. *ACS NANO.* 2011;12: 10041-  
6 10046.
- 7 [21] Chen X, Xu S, Yao N and Shi Y: 1.6 V Nanogenerator for Mechanical Energy Harvesting  
8 Using PZT Nanofibers. *Nano Lett.* 2010;10: 2133-2137.
- 9 [22] Jeong CK, Park KI, Ryu J, Hwang GT and Lee KJ: Large- Area and Flexible Lead-Free  
10 Nanocomposite Generator Using Alkaline Niobate Particles and Metal Nanorod Filler.  
11 *Adv Funct Mater.* 2014;24: 2620-2629.
- 12 [23] Xu S, Yeh YW, Poirier G, McAlpine MC, Register RA and Yao N: Flexible Piezoelectric  
13 PMN-PT Nanowire-Based Nanocomposite and Device. *Nano Lett.* 2013;13: 2393-2398.
- 14 [24] Sen S and Mishra SK: Electrical behavior of PMN-PT-PVDF nanocomposite. *J Phys D:*  
15 *Appl Phys.* 2008;41: 165305.
- 16 [25] Hwang GT, Park H, Lee JH, Oh S, Park KI, Byun M, Park H, Ahn G, Jeong CK, No K,  
17 Kwon H, Lee SG, Joung B and Lee KJ: Self-Powered Cardiac Pacemaker Enabled by  
18 Flexible Single Crystalline PMN- PT Piezoelectric Energy Harvester. *Adv Mater*  
19 2014;26: 4880-4887.
- 20 [26] Promsawat M, Watcharapasorn A, Ye ZG and Jiansirisomboon S: Enhanced Dielectric  
21 and Ferroelectric Properties of  $\text{Pb}(\text{Mg}_{1/3}\text{Nb}_{2/3})_{0.65}\text{Ti}_{0.35}\text{O}_3$  Ceramics by ZnO  
22 Modification. *J Am Ceram Soc.* 2015;98: 848-854.
- 23 [27] Niu R, Gong J, Xu DH, Tang T and Sun ZY: The Effect of Particle Shape on the Structure  
24 and Rheological Properties of Carbon-based Particle Suspensions. *Chin J Polym. Sci.*  
25 2015;33: 1550-1561.

- 1 [28] Gong H, Zhang Y, Quan J and Che S: Preparation and properties of cement based  
2 piezoelectric composites modified by CNTs. *Curr Appl Phys.* 2011;11: 653-656.
- 3 [29] Kondawar SB, Dahegaonkar AD, Tabhane VA and Nandanwar DV: Thermal and  
4 frequency dependence dielectric properties of conducting polymer/ fly ash composites.  
5 *Adv Mat Lett.* 2014;5: 360-365.
- 6 [30] Du P, Lin X and Zhang X: Dielectric constants of PDMS nanocomposites using  
7 conducting polymer nanowires. *Proc Int Conf on Solid- State Sensors, Actuators and*  
8 *Microsystems (TRANSDUCERS).* 2014;11: 645-648.
- 9 [31] Romasanta LJ, Hernández M, López-Manchado MA and Verdejo R: Functionalised  
10 grapheme sheets as effective high dielectric constant fillers. *Nanoscale Res Lett.* 2011;6:  
11 508.
- 12 [32] Park KI, Xu S, Liu Y, Hwang GT, Kang SJL, Wang ZL and Lee KJ: Piezoelectric BaTiO<sub>3</sub>  
13 Thin Film Nanogenerator on Plastic Substrates. *Nano Lett.* 2010;10: 4939-4943.
- 14 [33] Babu I, Hendrix MMRM and With GD: PZT-5A4/PA and PZT-5A4/PDMS piezoelectric  
15 composite bimorphs. *Smart Mater Struct.* 2014;23: 025029.
- 16 [34] Sharma SK, Gaur H, Kulkarni M, Patil G, Bhattacharya B and Sharma A: PZT-PDMS  
17 composite for active damping of vibrations. *Compos Sci Technol.* 2013;77: 42-51.

18

19

20

21

22

1  
2  
3  
4  
5  
6  
7  
8  
9  
10  
11  
12  
13  
14  
15  
16  
17  
18  
19  
20  
21

**Figure captions**

**Fig. 1** (a) Schematic of layered CNTs-added PMNT/PDMS nanocomposite and (b) showing high flexibility of the composite.

**Fig. 2** XRD patterns of monolithic PMNT particles and PDMS polymer, and a CNTs-added PMNT/PDMS nanocomposite.

**Fig. 3** SEM images of microstructures of (a) cross-section (b) an agglomerated PMNT particles (c) CNTs bridging PMNT particles and PDMS polymer of a layered CNTs-added PMNT/PDMS nanocomposite and (d) tomographic of the particles distributed in the polymer phase using synchrotron X-ray tomography.

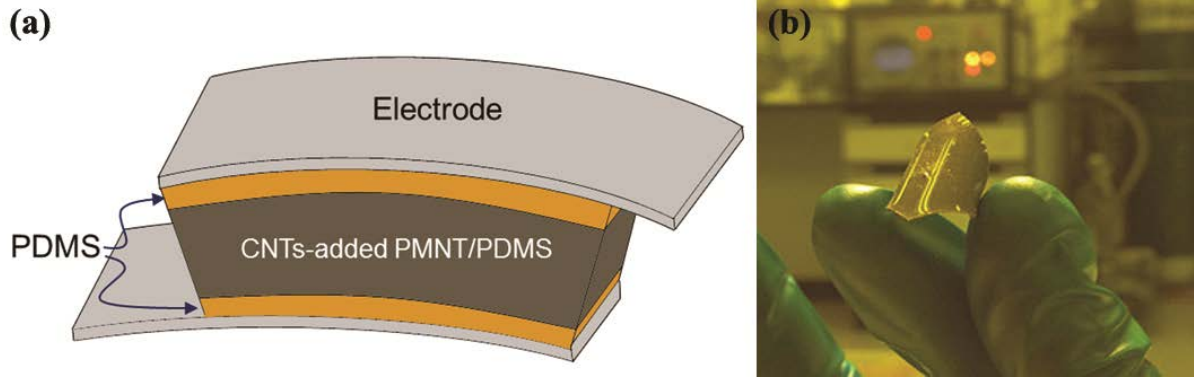
**Fig. 4** Energy dispersive X-ray spectra of (a) CNTs phase and (b) PMNT phase indicated by arrows in the CNTs-added PMNT/PDMS nanocomposite.

**Fig. 5** Frequency dependence of dielectric constant (black line) and dielectric loss (red line) of CNTs-added PMNT/PDMS nanocomposites.

**Fig. 6** Cycling output (a) voltage and (b) current under an applied mechanical force of 300 N of CNTs-added PMNT/PDMS nanocomposite.

1

2 Fig. 1

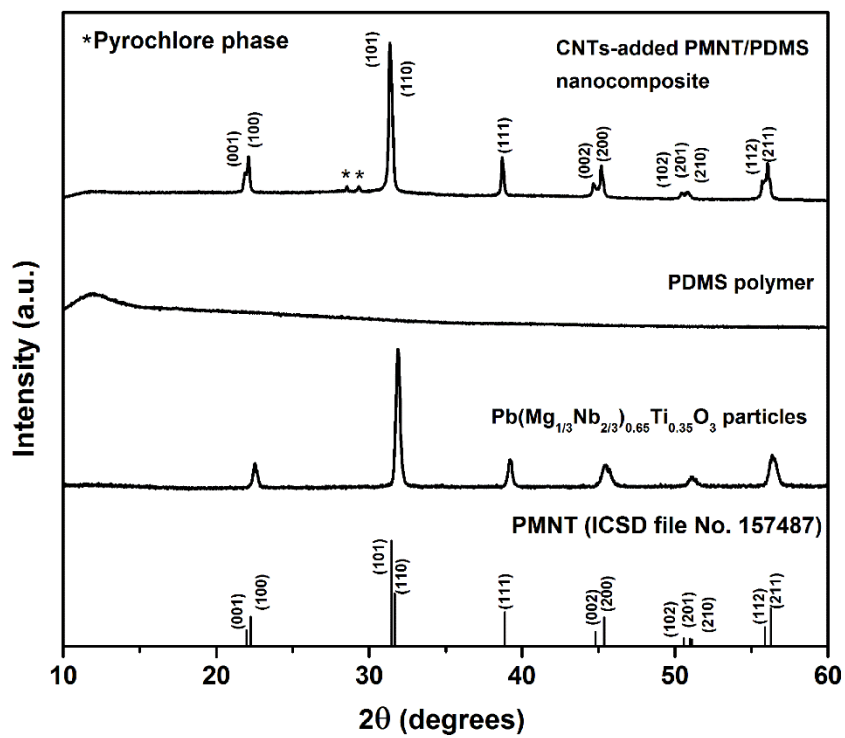


3

4

5

6 Fig. 2



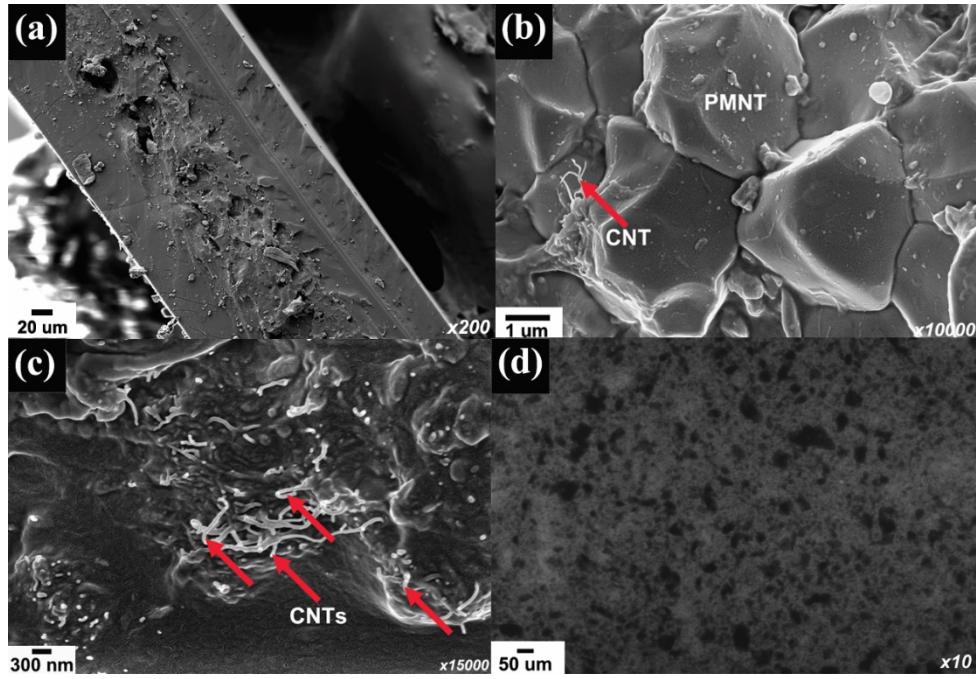
7

8

9

1

2 Fig. 3

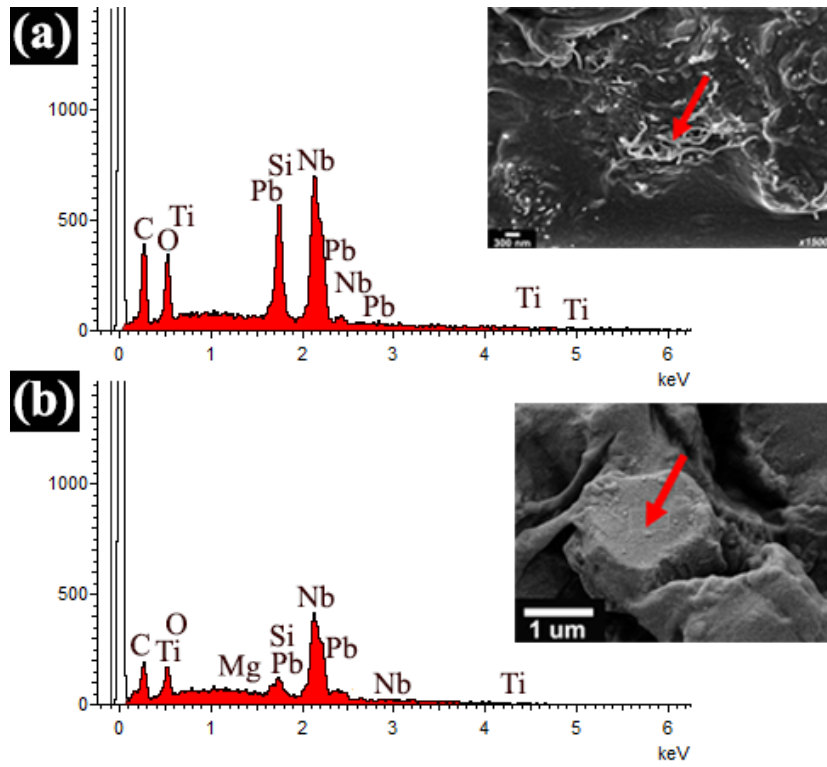


3

4

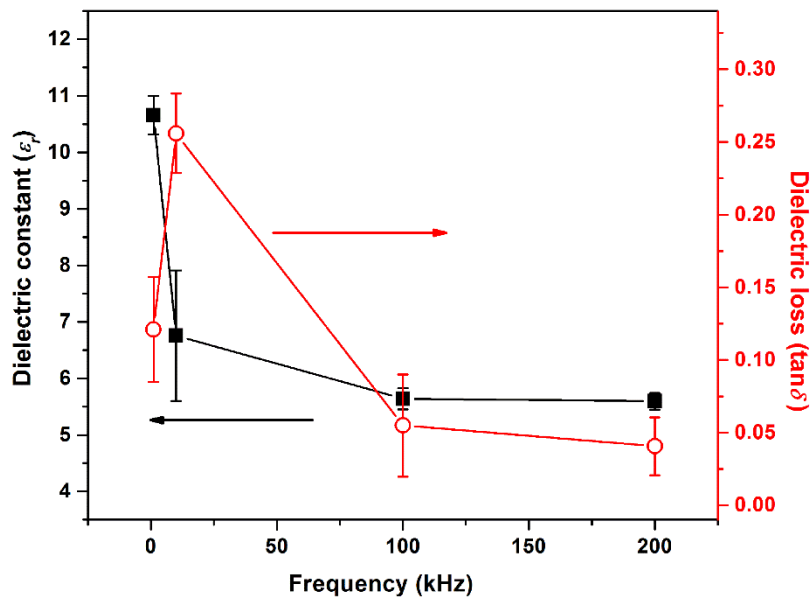
5 Fig. 4





1

2 Fig. 5



3

4 Fig. 6

